

Machine Vision Based Assessment of Fall Color Changes in Apple Trees: Exploring Relationship with Leaf Nitrogen Concentration

Achyut Paudel^a, Jostan Brown^b, Priyanka Upadhyaya^a, Atif Bilal Asad^a, Safal Kshetri^a, Manoj Karkee^a, Joseph R. Davidson^b, Cindy Grimm^b, Ashley Thompson^c

^aBiological Systems Engineering Department, Center for Precision and Automated Agricultural System, Washington State University, Prosser, 99350, WA, USA

^bCollaborative Robotics and Intelligent Systems Institute, Oregon State University, Corvallis, 97331, OR, USA

^cMid-Columbia Agricultural Research and Extension Center, Oregon State University, Hood River, 97031, OR, USA

Abstract

Apple trees being deciduous trees, shed leaves each year which is preceded by the change in color of leaves from green to yellow (also known as senescence) during the fall season. The rate and timing of color change are affected by the number of factors including nitrogen (N) deficiencies. The green color of leaves is highly dependent on the chlorophyll content, which in turn depends on the nitrogen concentration in the leaves. The assessment of the leaf color can give vital information on the nutrient status of the tree. The use of a machine vision based system to capture and quantify these timings and changes in leaf color can be a great tool for that purpose.

This study is based on data collected during the fall of 2021 and 2023 at a commercial orchard using a ground-based stereo-vision sensor for five weeks. The point cloud obtained from the sensor was segmented to get just the tree in the foreground. The study involved the segmentation of the trees in a natural background using point cloud data and quantification of the color using a custom-defined metric, *yellowness index*, varying from -1 to +1 (-1 being completely green and +1 being completely yellow), which gives the proportion of yellow leaves on a tree. The performance of K-means based algorithm and gradient boosting algorithm were compared for *yellowness index* calculation. The segmentation method proposed in the study was able to estimate the *yellowness index* on the trees with $R^2 = 0.72$. The results showed that the metric was able to capture the gradual color transition from

green to yellow over the study duration. It was also observed that the trees with lower nitrogen showed the color transition to yellow earlier than the trees with higher nitrogen. The onset of color transition during both years aligned with the 29th week post-full bloom.

Keywords: Fall Color Change, Machine Vision in Agriculture, Point Cloud Segmentation, Precision Nitrogen Management, Machine Learning in Agriculture

1. Introduction

High-density apple orchards (Figure 1) are becoming increasingly popular due to their potential for increased fruit production (Majid et al., 2018; Rallo et al., 2013). However, managing these dense orchards presents unique challenges, particularly in terms of assessing individual tree needs and making precise management decisions. Each tree within an orchard is a distinct entity with its specific requirements for water, nutrients, and other inputs (Aggelopoulou et al., 2010; James A. Taylor et al., 2007). This variability can be caused by multiple factors including spatial variation in soil properties like texture, depth, slope, and microbial activities (Aggelopoulou et al., 2010, 2011; Umali et al., 2012; Cho, 2010; Parkin, 1993). Ignoring these individual requirements can lead to suboptimal inputs, negatively impacting tree growth, yield, and fruit quality (Klein et al., 1989; Neilsen et al., 2009).

Traditional orchard management often relies on data collected from a limited sample of trees to represent the entire orchard. However, this method lacks precision due to inherent spatial variations within orchards, as highlighted in various studies (Ferguson and Triggs, 1990; Wulfsohn et al., 2012; Arnó et al., 2017). Nitrogen (N) plays a crucial role in orchard management and has impacts on plant growth, health, and fruit quality (Sanchez et al., 1995). Typically, nitrogen requirements for trees are assessed by visually analyzing canopy features like shoot length, density, and leaf color. Although this method provides insights into vital canopy characteristics, it remains subjective and exhibits considerable variability.

Nevertheless, seasoned experts often possess a keen understanding of a tree's nutritional status based on its visual appearance, honed through years of experience. A more informed



Figure 1: A typical commercial high-density apple orchard in Washington, USA

approach involves laboratory based leaf and soil nitrogen measurement, which provides higher accuracy but demands significant time and expense ([Baret and Fourty, 1997](#)). Both of these methods, however, focus on a sample of trees within the orchard, limiting the possibility of individual tree-level management. These problems in the current way of assessment highlight the necessity of a quick and reliable way of nitrogen assessment of the trees ([Cheng and Schupp, 2004a](#)). Understanding the parameters that experts use to assess tree nutritional status is crucial, and employing a machine vision system can aid in achieving this goal.

Canopy color, especially during the autumn color changes and leaf shedding is an important parameter for assessing the nitrogen level in the apple trees. A greener canopy with vigorous growth is often correlated with a tree having high nitrogen and a yellower and less vigorous canopy is often associated with trees with low nitrogen ([Raese et al., 2007](#); [Lee,](#)

2002). Leaf color strongly corresponds to leaf chlorophyll content, which, in turn, is closely tied to nitrogen content (Ali et al., 2012; Baret and Fourty, 1997; Treder et al., 2016; Rorie et al., 2011; Ye et al., 2020). Chlorophyll reflects the light in the green spectrum and thus is responsible for the green coloring of the leaves (National Geographic). Often, trees with very high nitrogen remain green until the end of the season. In deciduous trees like apples, the nitrogen present in leaves relocates to the woody regions during autumn for storage and supporting spring growth (Murneek and Logan, 1932; Spencer, 1973; Neilsen and Neilsen, 2002). The timing and pace of leaf color change could be influenced by external stressors like temperature and humidity, or internal factors such as nutrient deficiency (Aguëra et al., 2010; Wingler et al., 2009). Machine vision can be a great tool to capture and quantify these canopy features that are visually observed to effectively identify nitrogen stress in trees, offering a swift and reliable alternative to current nitrogen assessment methods.

Machine vision techniques have been extensively used to acquire various canopy-level features and stresses in the crop (Wang et al., 2023; Paudel et al., 2022; Wachs et al., 2010; Wang et al., 2018; Kang et al., 2023; Upadhyaya et al., 2023). Ongoing efforts aim to characterize diverse aspects such as canopy density (Mahmud et al., 2021; Paudel et al., 2023), tree trunk cross-sectional area (Wang et al., 2023), and canopy color (Naschitz et al., 2014) in fruit trees. Additionally, several studies have utilized machine vision to quantify leaf color and correlate it with tree nutritional status (Treder et al., 2016; Putra and Soni, 2020; Ma et al., 2018). While different sensors like RGB, multispectral, and hyperspectral cameras have linked image data to nitrogen or chlorophyll content, most studies have been confined to controlled environments, lacking representation of external orchard conditions.

A notable gap exists in research that tracks leaf color changes over time, offering insights into the evolving pattern of tree color changes. This study addresses this void by tracking apple trees over five weeks, quantifying their color changes within a natural orchard environment using machine vision. Specifically, the study aims to pursue the following research objectives:

1. Development of a machine vision-based technique to quantify foliage color during late fall.
2. Investigation of the relationship between foliage color in a tree and its foliar nitrogen concentrations.

The rest of the paper is structured into three sections. Section 2 details the data collection and processing methodologies. Section 3 delves into the results, offering insightful interpretation and pertinent discussion surrounding their emergence. Finally, Section 4 summarizes the key findings with discussions about the current limitations and future potentials.

2. Materials and Methods

The overall data collection and processing methodologies used in this study are shown in Figure 2. Further detail about each step has been explained in the subsequent sections of the paper. The study consisted of collecting data throughout the fall season for multiple weeks during the years 2021 and 2022. The processed point cloud of the trees were then segmented into yellow and green foliage and a metric - *yellowness index* was used to quantify the color of the trees. The color of the tree was then correlated to the leaf nitrogen content during each year and the patterns were analyzed.

2.1. Data Collection

The data for this study was collected over a period of five weeks, spanning the fall seasons of 2021 (from October 13 to November 14) and 2023 (from October 20 to November 17). Data was collected in a commercial orchard (Yakima Valley Orchard) in Prosser, WA (Figure 3) on Jazz™ apple trees during senescence (when the leaves started to change the colors from green to yellow (Figure 4)). The trees data were scattered across 17 rows. The data was collected using a commercial stereo-vision based camera (Zed2i (Stereolabs, Paris, France)) mounted on a utility vehicle (Figure 3b). The trees were trained in a tall spindle system with

a vertical wall (Figure 3c). The camera was mounted about 7 feet from the ground to ensure the majority of the canopy was visible. An SVO file (Stereolabs file format) with all the metadata including the camera parameters, images, and sensor data was recorded

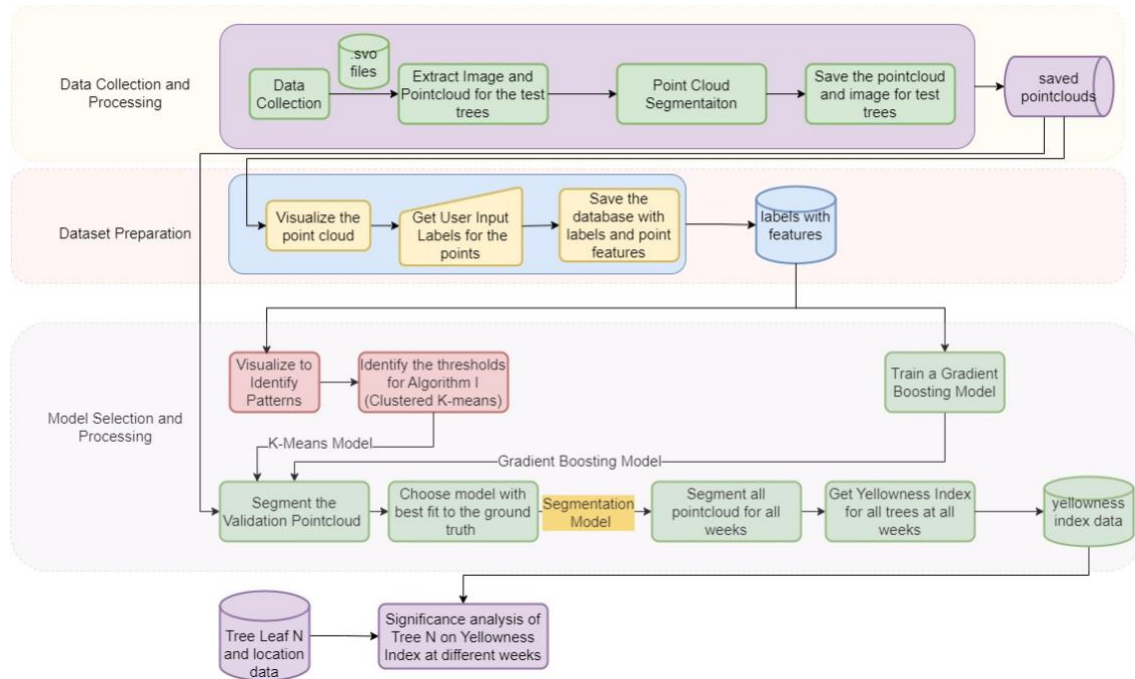


Figure 2: Overall Data collection and processing method for the study. Each light colored box represent a distinct process and has been described further in subsequent sections.

for each row during data collection at a resolution of 2208 x 1242 pixels and extracted later during data processing. The data collection was done through zed package (Stereolabs, 2023) for Robot Operating System (ROS) (Quigley et al., 2009). A custom ROS node (Quigley et al., 2009) was written to record user input, including tree numbers, when the vehicle was in front of the desired tree. Images and pointcloud for each tree were later extracted based on timestamp matching between frames and user input, with the frame with the closest timestamp being selected. During processing, the RGB and co-registered pointcloud were extracted for each test tree.

2.2. Point Cloud Processing and Segmentation

2.2.1. Foreground Tree Segmentation

The initial data acquired through the stereovision sensor was noisy and required further refinement. An initial step involved applying a color threshold of 153 to the blue channel to filter out pixels corresponding to the sky. Subsequently, a distance threshold of 3 meters

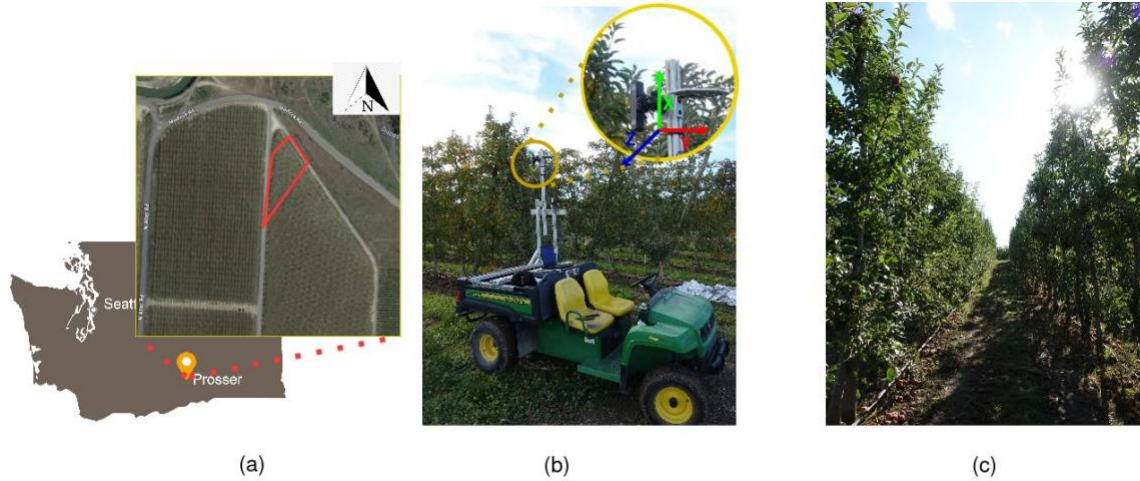


Figure 3: (a) Washington state map with Prosser shown, zoomed portion shows location of an orchard,(b) Ground vehicle with a camera mounted on top (zoomed portion shows camera and axes orientations), and (c) A representative orchard row with trees trained into a vertical wall system.

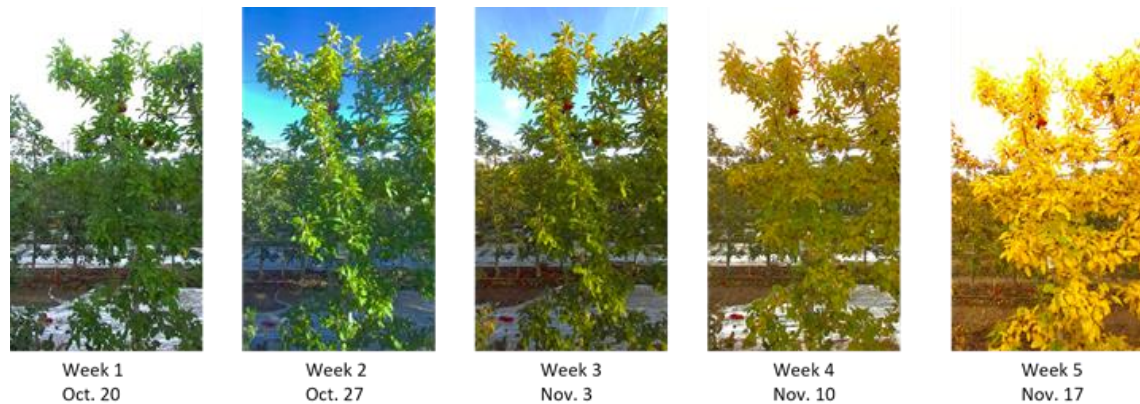


Figure 4: Images of the same tree during different weeks of the data collection. The dates below represent the exact dates when the data was collected in 2023. The foliage can be seen gradually changing from green to yellow.

along the Z-axis(along the depth axis), was implemented. Consequently, the resulting point cloud consisted of points mostly from the foreground tree, with some residual points from the ground. To eliminate the undesirable ground points, the points within 50 centimeters

above the lowest x-value (along the height of the tree) were excluded. The resulting point cloud was downsized by selecting every tenth point, effectively reducing its size while preserving essential information for subsequent analysis.

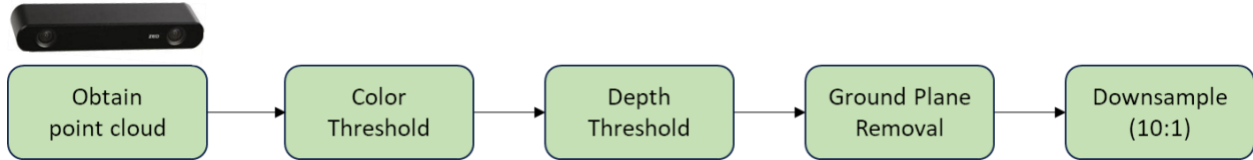


Figure 5: Schematic for point cloud segmentation and downsampling process used in the study

2.2.2. Color Segmentation and clustering

The point cloud obtained from step 2.2.1 consisted of points from the foreground tree, and could be broadly categorized into yellow leaves, green leaves, and the trunk. Data collection spanned multiple weeks, capturing the tree’s seasonal shift during the fall color change, depicted in Figure 4. Given the diverse collection periods and varying lighting conditions affecting RGB intensities, alternative color spaces like HSV (Figure 6a) and CIE-Lab* (Figure 6b and c) were opted for due to their reduced susceptibility to lighting fluctuations. In the HSV space, hue remains unaffected by varying light, while in the CIE-Lab* space, the a^* and b^* values correspond respectively to red-green and blue-yellow colors. The initial RGB image was converted to the CIE-La*b* (Lab) space using a standard D65 illuminant through the scikit-image library (Van der Walt et al., 2014).

The transition of the trees from green to yellow color was noticeable in both HSV and La*b* space (Figures 6a and 6b,c). A probability density plot for the hue space across the weeks illustrated a decline from approximately 110 degrees in week 1 to about 50 degrees in week 6, signifying the shift from green to yellow. A similar trend was visible in the probability density plots for a^* and b^* in the La*b* space. Both a^* and b^* showed a slight increase as the weeks progressed, corresponding to a color change from green to yellow.

The transition in tree colors was apparent qualitatively, but a robust quantitative approach was needed to precisely quantify them. To achieve this, the study focused towards

categorizing individual points into distinct groups of yellow leaves, green leaves, or the trunk. Qualitative analyses using K-means clustering over multiple samples in both the La^*b^* and HSV color spaces showed that the La^*b^* space performed better in distinguishing yellow and

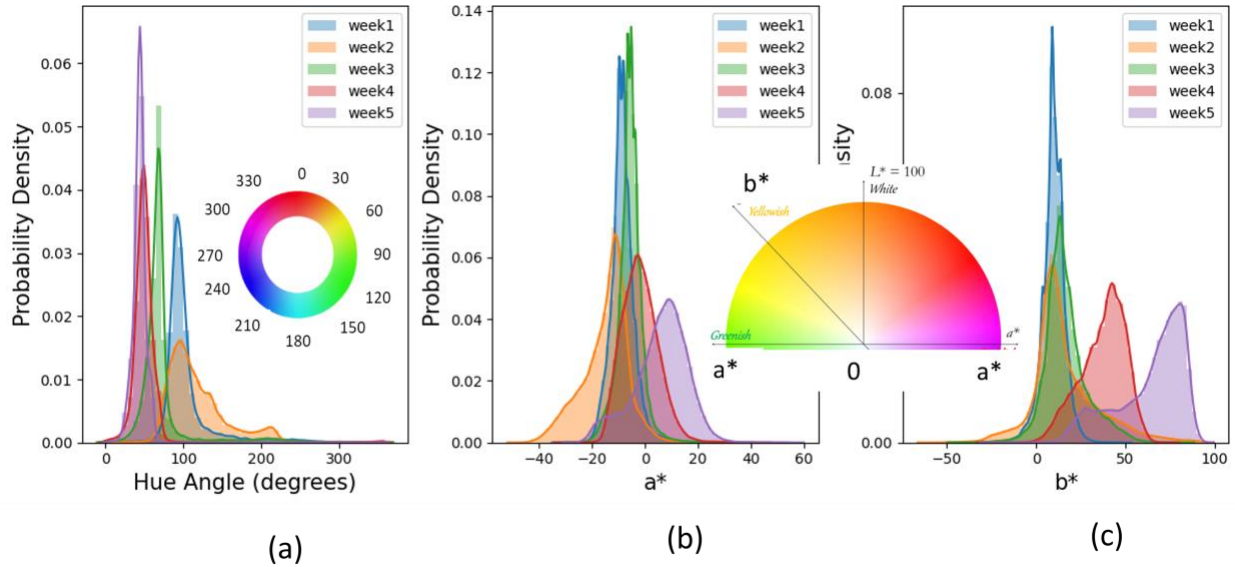


Figure 6: Distribution of a) Hue angles and b) a^* and c) b^* values for one of the sample trees during the five-week study period of 2023. The color chart shows the color associated with different values for (a) hue angles, (b) (Thompson, 2017) a^* , and b^* . The hue angle decreased in a) and a^* and b^* increased in b) and c) as the weeks progressed during the study all signifying the shift from green to yellow.

green pixels as separate classes. Consequently, the subsequent analysis was conducted within the La^*b^* color space. To cluster the point cloud, a k-means algorithm was applied, initially grouping the points into 20 clusters. A threshold for the cluster center was set in both the a^* and b^* space, to merge these clusters into three distinct classes: *Yellow*, *Green*, and *Trunk*. The *Yellow* cluster encompassed foliage that had transitioned to yellow, while the *Green* cluster comprised foliage that retained its green color. The *Trunk* cluster included points from the trunk, branches, background soil, and some brown leaves. A detailed breakdown of the clustering process is outlined in Algorithm 1.

Algorithm 1: Clustering of Point Cloud

Input: Point cloud from stereovision system , P

Output: Clustered Point cloud–3 groups, Green, Yellow, Trunk

```
1      $n$  = initial number of cluster (integer)
2     K-Means Clustering using  $a$ ,  $b$  values into  $n$  clusters ( $c$ )
3     Green cluster( $c_g$ ) = 0; Yellow cluster( $c_y$ ) = 0; Trunk cluster ( $c_t$ ) = 0
4     for  $i$  in range( $n$ ) do
5         if  $c_{g_{amin}} < c_i(a) < c_{g_{amax}}$  and  $c_{g_{bmin}}c_i(b) < c_{g_{bmax}}$  then
6              $C_g = C_g + C_i$ ;
7         else if  $c_{y_{amin}} < c_i(a) < c_{y_{amax}}$  and  $c_{y_{bmin}}c_i(b) < c_{y_{bmax}}$  then
8              $C_y = C_y + C_i$ 
9         else if  $c_{t_{amin}} < c_i(a) < c_{t_{amax}}$  and  $c_{t_{bmin}}c_i(b) < c_{t_{bmax}}$  then
10             $C_t = C_t + C_i$ 
11        end
12    end
13    return  $C_g, C_y, C_t$ 
```

In the aforementioned algorithm, the manual setting of threshold values for a^* and b^* required multiple iterations to identify optimal values suitable across the data throughout the weeks. To standardize this process, a methodology involving manual user input labels was implemented to obtain a labeled dataset. A custom Python program (Figure 7), using the Open3D library (Zhou et al., 2018), was developed to label the point cloud. This interactive program allowed users to choose between three labels - 'Green', 'Yellow', and 'Trunk' and manually select the points belonging to these labels. Trees were randomly sampled throughout the entire data collection period, and the labels along with the characteristics of the points were recorded to create the dataset.

To visualize the difference between groups, a distribution plot of the a^* , and b^* spaces was

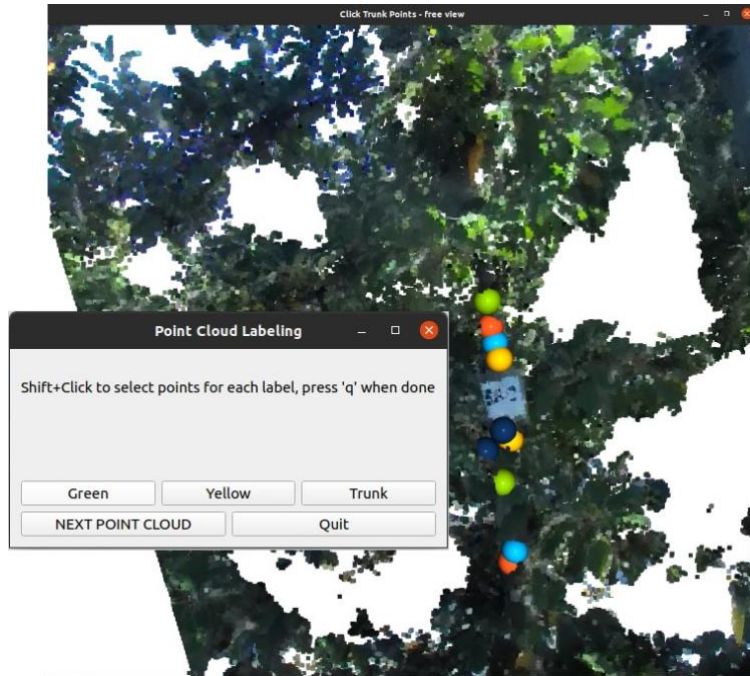


Figure 7: Custom program to select the points belonging to multiple classes - Green, Yellow, and Trunk. This instance showed an interactive window where the user selected points belonging to the trunk. The features of the points - including a^* , b^* , R , G , B , and their eigenvector and eigenvalues were recorded into a spreadsheet for further analysis.

created (Figure 8). These plots provided strategic reference points for selecting threshold values. For the 2023 dataset, the threshold values for a^* and b^* were determined as follows: $a^* < -10$, $0 < b^* < 25$ for 'Green', $b^* > 45$ for 'Yellow', and $a^* > 0$, $0 < b^* < 50$ for 'Trunk'. While K-means clustering, being an unsupervised method, doesn't necessitate user inputs for training data and attempts to identify inherent clusters in the dataset, it comes with certain drawbacks. The method's main limitations include longer computation times due to the need to process all points and its reliance on random initialization, potentially leading to different solutions with each run.

An alternative approach utilized a gradient boost classifier, an ensemble learning technique that combines multiple weak learners (typically decision trees) to create a stronger, more robust model (Bartlett et al., 1998). It sequentially builds new models, focusing on correcting the errors made by the previous ones, ultimately producing a more

accurate and powerful predictive model (Natekin and Knoll, 2013). The gradient boost classifier model

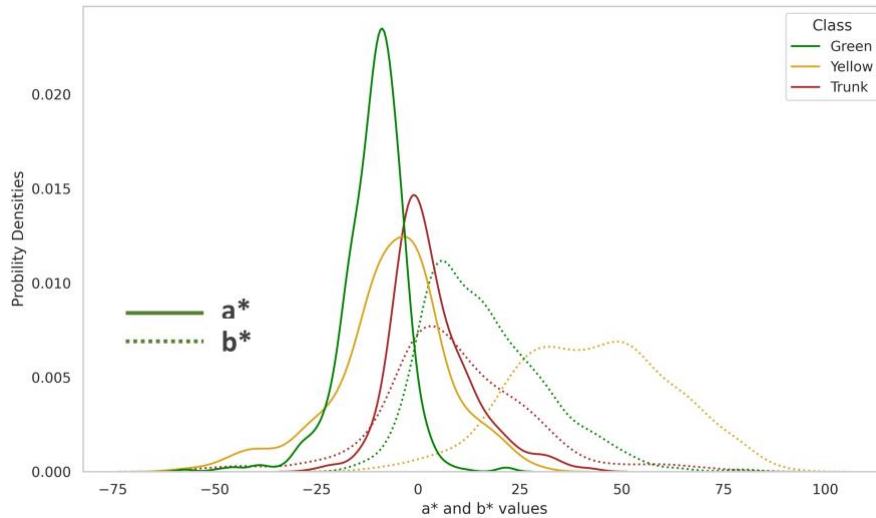


Figure 8: a^* and b^* values in CIE- $L^*a^*b^*$ space during different weeks for points belonging to green, yellow, and trunk classes in 2023. The solid lines represent a^* values, and dotted lines represent b^* values, different colors represent different classes.

was created using scikit-learn (Van der Walt et al., 2014). The dataset was divided into 80% training and 20% testing datasets. The model required different hyperparameters to be tuned. A strategic way of varying hyperparameters was chosen with the model having the highest accuracy on the test data being chosen. The hyperparameter *learning rate* was varied between 0.1-1, *max depth* was varied between 1-5, and *n estimator* was varied between 100-1000 and their performance on training and test dataset was analyzed.

The outputs from both Algorithm 1 and the Gradient Boosting method provided labels—'Green', 'Yellow', or 'Trunk'—for each point in the point cloud. Following the point grouping, a metric, *yellowness index*, was used to quantify the extent of yellowing within the tree. The *yellowness index*, calculated using Equation 1, represents the normalized ratio between yellow and green points in the dataset, with values ranging between -1 and +1. A value of -1 indicates that the tree was entirely green, while a value of +1 signifies complete yellowing.

$$yellowness\ index = \frac{y-g}{y+g} \quad (1)$$

where, y = number of points with 'Yellow'

label (c_y) g = number of points in 'Green' label

(c_g)

To validate the findings of the study, 50 trees were randomly selected and defoliated between the second and fourth trellis wires (Figure 9). The leaves removed from each tree were collected in a bag and then later segregated into separate groups. Each leaf for individual trees was manually sorted into two groups, 'Green' if more than half of the leaf was green, and 'Yellow' if more than half was yellow (Figure 10). Two groups of yellow and green leaves were obtained from each validation tree. The precise weights of the yellow and green leaf groups were measured using a highly accurate Mettler PC 4000 (Mettler Toledo, Switzerland) weighing scale. The *yellowness index* value was computed for all validation trees using Equation 1. This value served as the ground truth to assess the models' performance. Both Algorithm 1 and Gradient Boosting were evaluated against the validation data, with the superior-performing model selected based on this evaluation.



Figure 9: The image of the tree before and after defoliation. The leaves from the tree between the second and fourth trellis wire from the bottom (shown in transparent red box) were defoliated and collected.

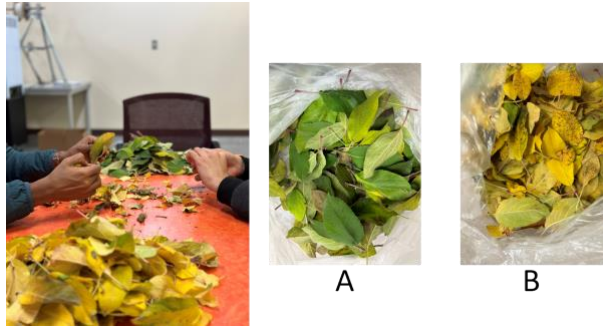


Figure 10: One instance of separation of the leaves based on the color. The leaves from each validation tree were separated into (A)Green and (B)Yellow groups, and weighed separately to calculate the *yellowness index*.

2.3. Relationship between Yellowness Index and Leaf Nitrogen Concentration

To investigate if the *yellowness index* had any relationship with the foliar nitrogen concentration on the trees, the *yellowness index* values were regressed against the leaf nitrogen concentration. The leaf nitrogen concentration were obtained using the standard Kjeldahl's method (Kirk, 1950) by collecting 50 fully grown mid-shoot leaves from each tree, at the end of the growing season (Late July in 2021 and early August in 2023). The leaf nitrogen concentration would show the average nitrogen status of the tree and has been linked with various factors like canopy growth and canopy color. There are different recommendations on a good nitrogen level for trees depending on the variety (Cheng and Schupp, 2004b; Cheng, 2010; Sallato, 2017; UniversityofArizona). The leaf nitrogen level of 2-2.4% was regarded as a good nitrogen level in this study for Jazz™apple trees based on these recommendations.

A one-way ANOVA analysis was conducted to examine the yellowness values across various weeks, classifying trees into either 3 or 5 groups according to their leaf nitrogen concentrations. In the 3-class classification, trees were categorized as 'Low'($N < 2\%$), 'Good'($2\% < N < 2.4\%$), and 'High'($N > 2.4\%$) . Meanwhile, the 5-class classification included 'VeryLow'($N < 1.7\%$), 'Low'($1.7\% < N < 2\%$), 'Good'($2\% < N < 2.4\%$), 'High'($2.4\% < N < 2.6\%$), and 'VeryHigh'($N > 2.6\%$) categories. The ANOVA analysis was followed up by a Tukey HSD posthoc analysis to

analyze the significant difference between pairs of groups if ANOVA showed a significant difference.

3. Results and Discussions

3.1. Tree Segmentation and Clustering

The images and point cloud of the tree obtained from Section 2.2.1 were saved and used during the processing. It was necessary that the point cloud was separated into green leaves and yellow leaves to quantify the yellowness in the tree. For that, two models were explored: a) Algorithm 1 and b) Gradient Boost classifier. Algorithm 1 was unsupervised and thus didn't need any manual input, except the threshold values which has been discussed in Section 2.2.2 and Figure 8. Gradient boost classifier, however, needed some training data and was trained on data collected as discussed in section 2.2.2. The hyperparameters *learning rate*, *max depth*, and *n estimator* were varied to identify the best hyperparameter for the model. The results of the model performance during hyperparameter tuning are shown in Figure 11. It can be seen that the model soon starts to overfit with higher performance on the training set, at the cost of reduced performance on the test set signifying the overfit of the model on the train set. The highest performing model on the test set had an accuracy of 78% on the test set with a learning rate of 0.1, maximum depth of 1, and a number of estimators as 100.

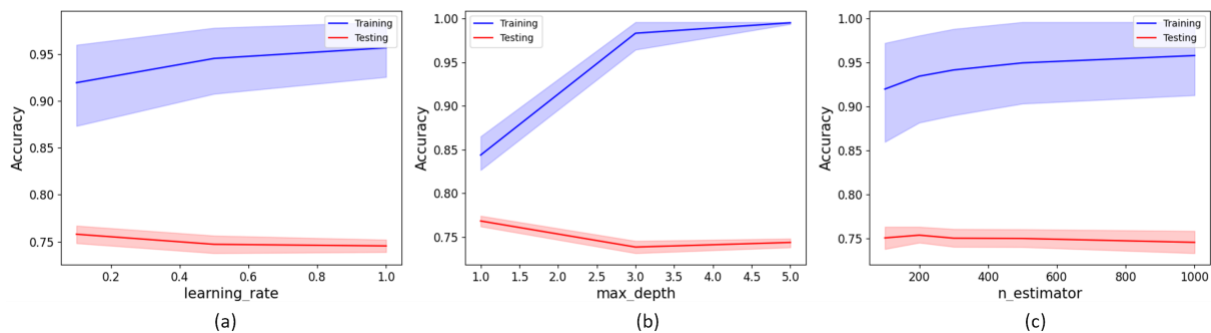


Figure 11: Variation of model accuracies with changing hyperparameters (a) Learning Rate, b) Maximum Depth of Tree, and c) Number of Estimators. The blue line denotes accuracies during training, while the red line represents accuracies during testing. The shaded regions around the lines illustrate the range of accuracies across different values of the other hyperparameters, with the indicated hyperparameter being held constant.

The best-performing Gradient Boost model was compared against Algorithm 1 to determine the superior method. The models were evaluated using the validation data, detailed in Section 2.2.2. Figure 12 shows both models' performance within cropped regions (between the second and fourth trellis wire) in a) and b). Further assessment involved computing the *Yellowness Index* from both the manual weight-based calculation and point cloud segmentation-based classification of the validation trees. As shown in Figure 13, both models displayed comparable classification accuracies on the validation data. However, Algorithm 1 exhibited significantly slower processing speeds compared to the Gradient Boosting method. On the same point cloud, Gradient Boosting processed approximately six times faster (with average segmentation time of 2.41 sec for Algorithm 1 and 0.39 sec for Gradient Boosting while running on 35 trees across multiple weeks). Consequently, Gradient Boosting was selected as the optimal model for subsequent point cloud segmentation. The model was run on pointcloud of all data trees across all weeks and the segmented pointcloud was also saved. Figure 14 demonstrates the results from the gradient boost segmentation model for a test tree during weeks 1, 3, and 5.

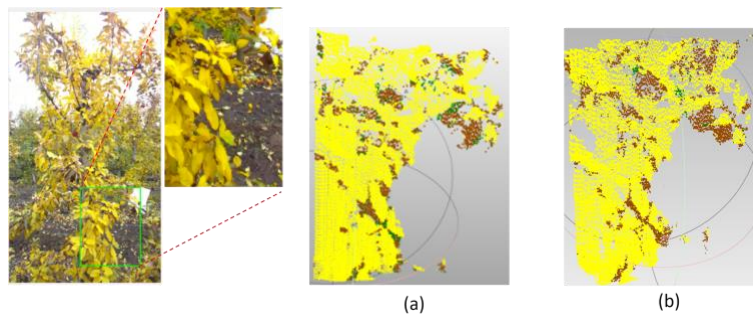


Figure 12: Segmented point cloud of the validation data. The region from the green rectangle was extracted and cropped image and point cloud from that region was obtained. The results from the segmentation models on the cropped point cloud are shown in a) Algorithm 1 and b) Gradient Boosting Classifier. The three colors in the point cloud represent three groups; green, yellow, and Trunk.

3.2. *Yellowness Index and Leaf Nitrogen Concentration*

The segmentation model was run for the point cloud of all the test trees during all weeks for the study duration. The model gave the labels for each point in the pointcloud as output.

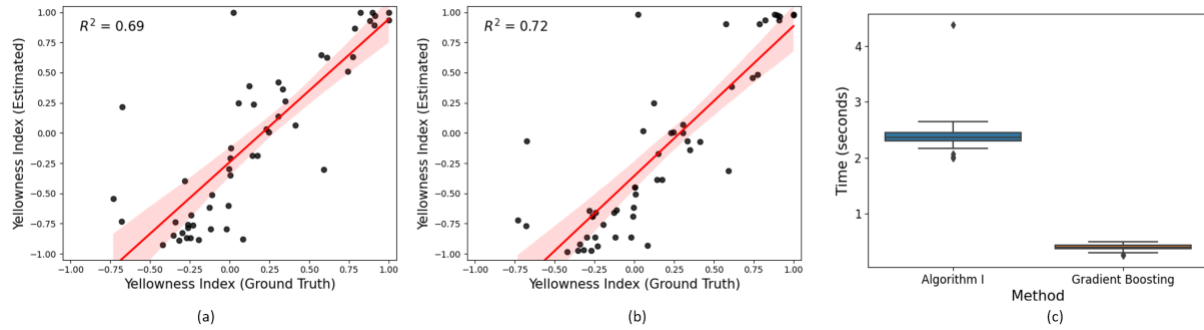


Figure 13: Performance of a) Algorithm 1 and b) Gradient boosting classifier on the validation dataset. The time taken for performing classification on thirty-five trees across multiple weeks for both models is shown in (c).

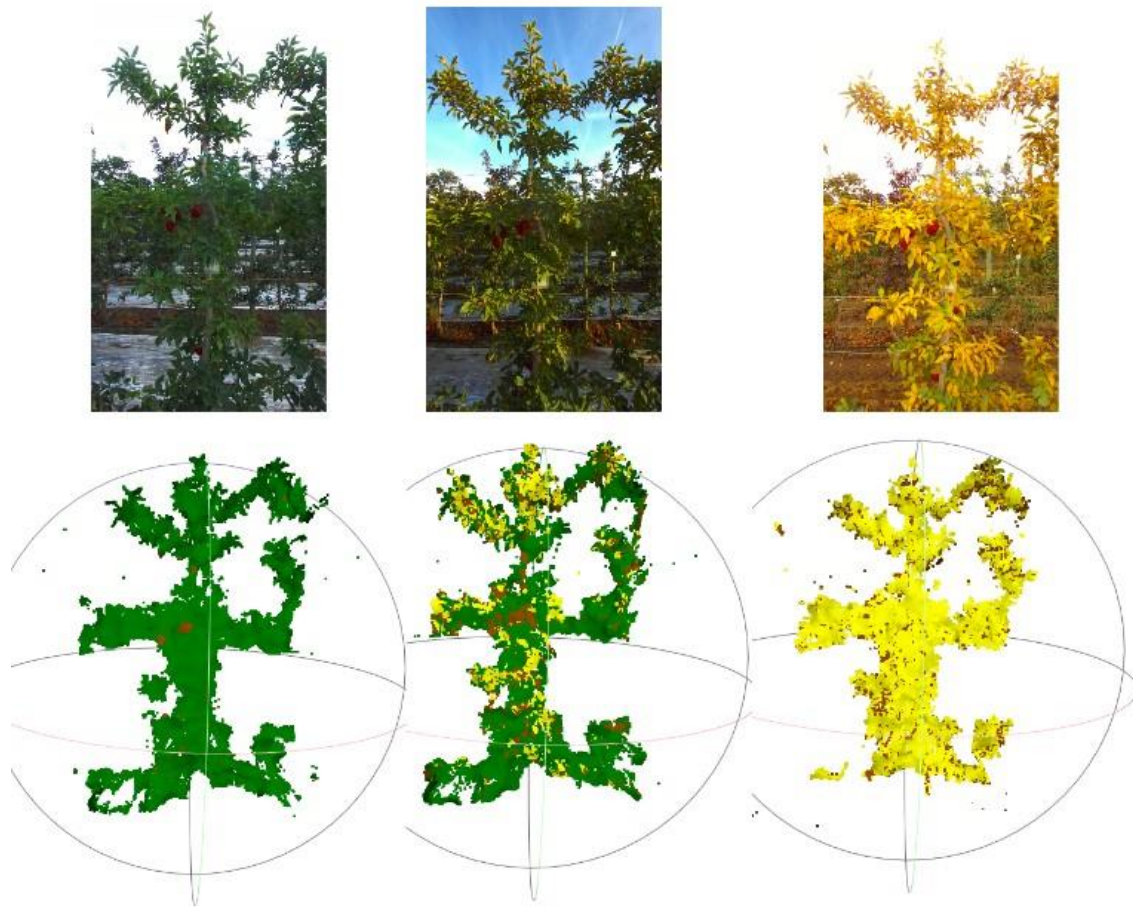
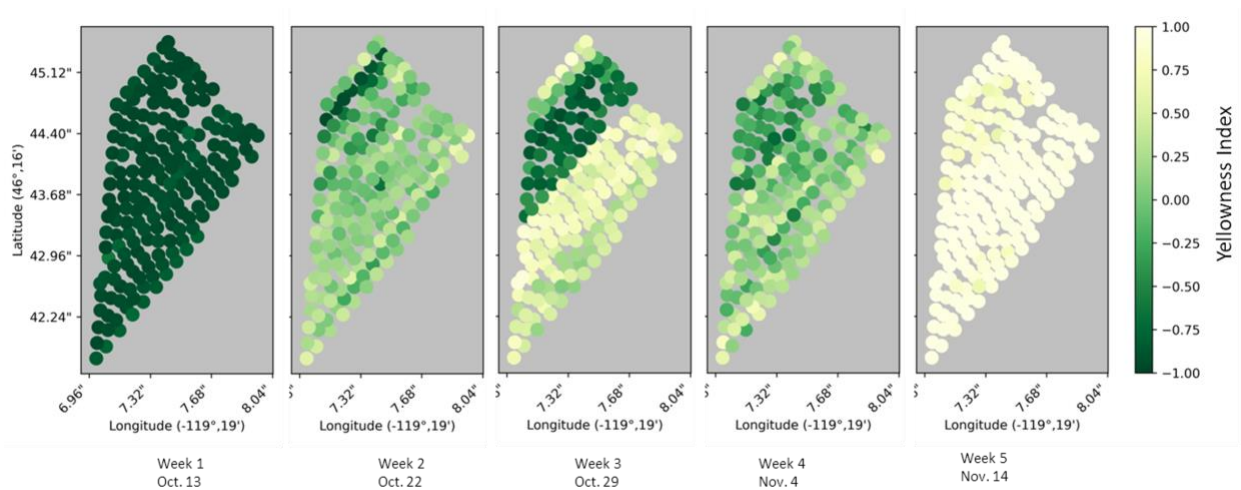


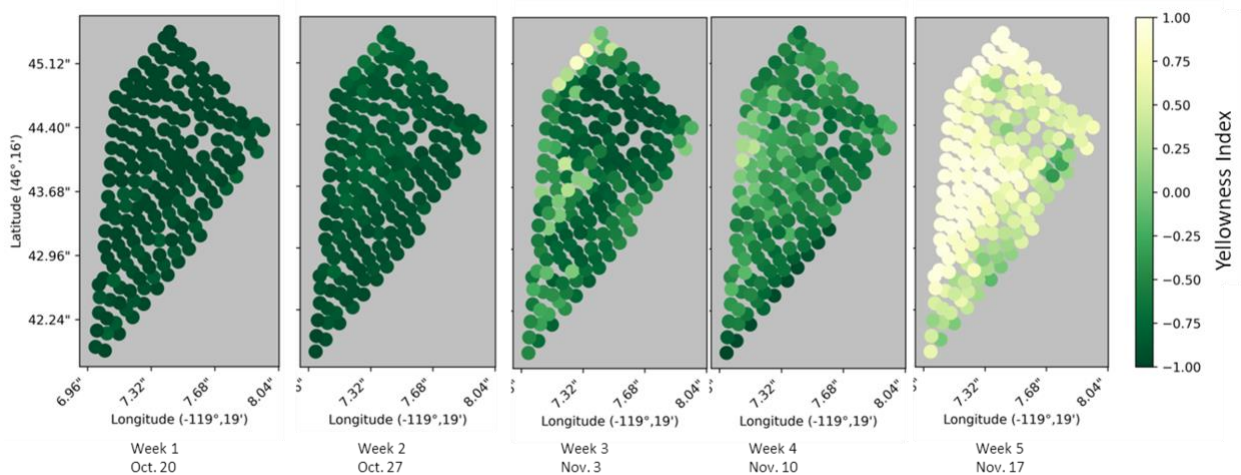
Figure 14: The images (top row) and segmented point cloud (bottom row) of a test tree during weeks 1, 3, and 5. The three colors in the point cloud represent three groups; green-green leaves, yellow-yellow leaves, and brown-trunk, branches and some leaves that have turned brown. After the clustering of yellow and green leaves in each tree, the *yellowness index* value was calculated for each tree for each week using equation 1. The *yellowness index* at different weeks were plotted into a spatial map with each tree's geolocation to further help visualize

the pattern of yellowing of the trees. Figure 15 a) and b) show the spatial variation in yellowing pattern across the trees in 2021 and 2023 respectively. The darker points in the map represent greener trees and the lighter points in the map represent yellower trees. A consistent trend of increasing *yellowness index* is noticeable as the weeks progress in both years. However, it was noticed that the yellowness trends was different between the years. In 2021, trees showed early transition to yellow in week 2 (around October 22), whereas in 2023, this change occurred later, nearly after three weeks (between week 4(November 10) and week 5(November 17)). This difference could potentially be attributed to relatively higher temperatures in 2021 compared to 2023 (Figure 16, AgWeatherNet) as shown by the cumulative growing degree days. Prior studies by De la Haba et al. (2014) and Kim et al. (2020) have highlighted the impact of higher temperatures on senescence, indicating that elevated temperatures can induce early senescence in foliage. Additionally, considering the full bloom dates—April 13 in 2021 and May 2 in 2023—almost three weeks apart, aligning with the timing difference in tree yellowing. In both cases, yellowing occurred approximately 29 weeks after full bloom. Combining temperature data with bloom dates could provide a more comprehensive understanding of the timing of fall color changes in apple trees.

To further explore the variation in color transformation, the correlation between leaf nitrogen concentrations and yellowness was investigated. Leaf nitrogen plays a pivotal role in regulating chlorophyll levels, which, in turn, influence leaf greenness (National Geographic; Ye et al., 2020; Rorie et al., 2011). A regression plot (Figure 17) was generated, plotting leaf nitrogen concentrations against the *yellowness index* across all weeks during both a)2021 and b)2023. The scatter plots were categorized into five groups based on leaf nitrogen concentrations, as outlined in Section 3.2. Higher nitrogen levels in trees correlated with



(a)



(b)

Figure 15: Spatial variation of *yellowness index* over the study duration in the orchard during a) 2021 and b) 2023. The color bar on the right indicates the yellowness level, with darker shade representing greener trees and lighter shade representing yellower trees.

lower *yellowness index* values for both years, suggesting extended retention of greenness in trees with greater nitrogen content compared to those with lower levels. This observation resonates with existing literature emphasizing that trees with higher nitrogen levels tend to maintain their green coloration longer. Additionally, various methods employed to estimate nitrogen content in leaves often rely on assessing leaf greenness (Shi et al., 2021; Wen et al., 2018; Li et al., 2022). The results indicate that the yellowness of trees at different weeks

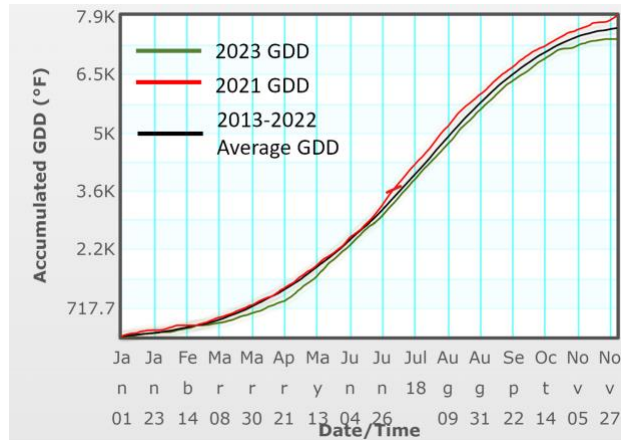
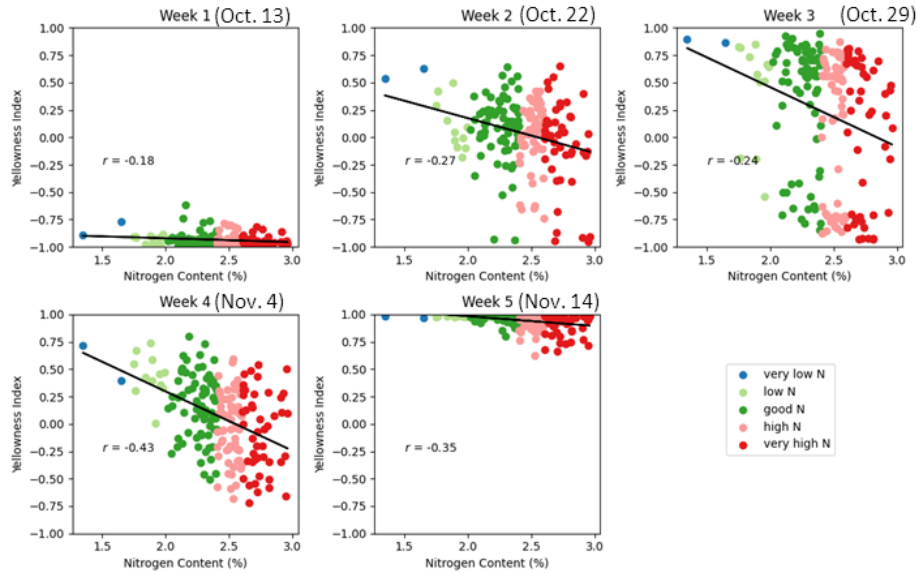


Figure 16: Growing degree days during 2021 and 2023 (AgWeatherNet). The red line shows the cumulative growing degree days for 2021 the green line shows that for 2023. The black line shows the average cumulative growing degree days between 2013 and 2022.

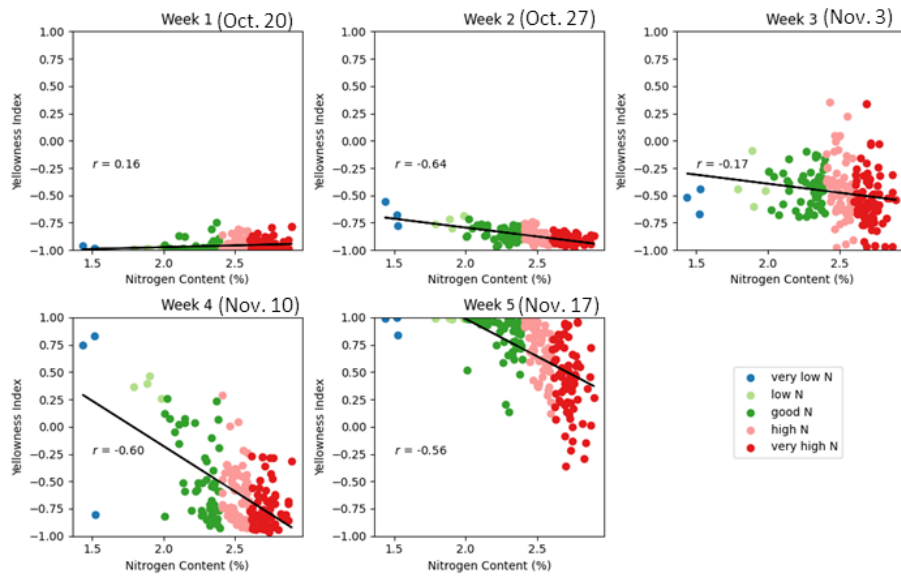
and the pattern in which they are changing can be an indicator of the nitrogen status in the tree.

The relationship of leaf nitrogen concentration on *yellowness index* can also be seen in Figure 18 which shows leaf N concentrations and *yellowness indices* of the trees in a spatial plot during week4 of 2021 and week5 of 2023. In both plots, red ellipses represent areas with higher leaf N and black ellipses represent areas with lower leaf N. It can be noticed in both these plots that the area with low leaf Nitrogen (right plots - black ellipses) has higher *yellowness indices* in the left plots. The area with high leaf Nitrogen in left plots (red ellipse) has lower *yellowness indices* i.e. greener. These findings suggest that the leaf N plays a role in determining the yellowness of the trees which have been correctly captured by the *yellowness index* metric.

To investigate potential differences in the *yellowness index* among trees exhibiting varying leaf nitrogen levels across different weeks during the season, a one-way ANOVA was performed, as detailed in Section 2.3. Trees were segregated into three and five classes based on their nitrogen levels (Section 2.3), and the disparities in group means were analyzed across different weeks in the study period. The analysis encompassed data from both 2023



(a)



(b)

Figure 17: Yellowness Index over weeks during the fall season of (a) 2021 and (b) 2023 in trees shown with Nitrogen % in the trees. (Very low N ($N < 1.7\%$), Low N ($1.7\% < N < 2.0\%$), Good N ($2\% < N < 2.4\%$), High N ($2.4\% < N < 2.6\%$), Very high N ($N > 2.6\%$). The dates on the plots show the date when the data was collected in 2021 and 2023.

and 2021 at both classification levels(3 and 5 groups). A significant difference between the group means existed in weeks 1, 2, 3, and 4 of 2021 and weeks 2, 4, and 5 of 2023, all at

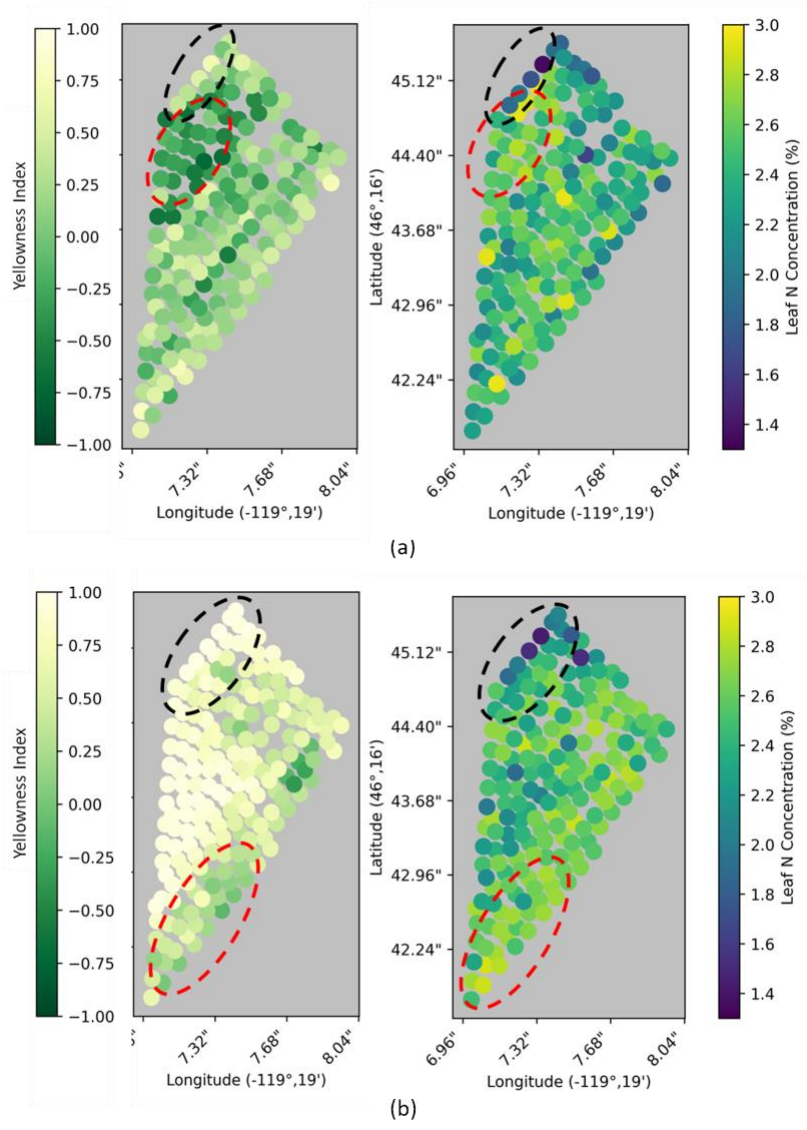


Figure 18: *Yellowness Index* (left plots) variation with leaf nitrogen concentrations (right plots) in (a) week 4 of 2021, and (b) week 5 of 2023. The colorbars on the left and right show the values of *yellowness index* and leaf nitrogen concentrations. The red ellipses show the sample areas with higher nitrogen concentrations, and the black ellipses show areas with lower nitrogen concentrations.

a significance level of $p < 0.05$. Subsequently, post hoc analysis via TukeyHSD tests at the same significance level was conducted, presenting the results in Table 1. Rows shown in the table indicate that there existed a significant difference in group means between values in Column Group 1 and Group 2 at the given week. These findings, categorized into both the 3-class and 5-class analyses, revealed a higher occurrence of significant differences between Group 1 and Group 2 during weeks 2 and 4 in 2023 and week 4 of 2021.

These findings underscore the significance of critical periods for distinguishing between trees with low and high nitrogen levels. The timing of these crucial periods appears to differ between years, as observed in data from two distinct years. To establish a more robust predictive method for identifying these significant timings, it's essential to consider various factors like growing degree days, precipitation, and average temperatures. The results from this study indicate that the machine vision system was able to identify the critical differences in the yellowing patterns of the trees and could be used as a predictor of nitrogen levels in apple trees.

Table 1: Post-hoc analysis (Tukey test) between trees at different N concentrations when divided into 3 and 5 classes based on leaf Nitrogen concentrations at a) 2021 and b) 2023. The given rows showed significant differences between Group 1 and Group 2 in the column during the given week at a significance level of $p < 0.05$.

		(a)		(b)					
		3 classes		5 classes		3 classes		5 classes	
		Group1	Group2	Group1	Group2	Group1	Group2	Group1	Group2
Week1				Low	Very_High				
Week2	Good	High							
Week3	Low	High	Low	Very_High					
	Good	High	Good	Very_High					
Week4	Low	Good	Low	High					
	Low	High	Low	Very_High					
	Good	High	Good	High					
			Good	Very_High					
Week2	Low	Good	Very_low	Good					
	Low	High	Very_Low	High					
	Good	High	Very_Low	Very_High					
			Low	Good					
			Low	High					
			Low	Very_High					
			Good	High					
			Good	Very_High					
Week4	Low	Good	Very_Low	Low					
	Low	High	Very_Low	High					
	Good	High	Very_Low	Very_High					
			Low	Good					
			Low	High					
			Low	Very_High					
			Good	High					
			Good	Very_High					
Week5	Low	Good	Very_Low	Low					
	Low	High	Very_low	Good					
			Very_Low	High					
			Very_Low	Very_High					

The outcomes and methodologies of this study offer a means to quantify tree color and determine tree nitrogen levels, crucial factors in guiding fertilizer applications. However, the system relies on machine vision, susceptible to variations in external lighting conditions. Nevertheless, recent advancements in machine vision sensors have addressed low-light

conditions using innovative techniques (Zhang et al., 2020, 2021). Deep learning methods have notably enhanced camera system resilience to diverse lighting environments (Li et al., 2021a,b). The algorithm employed in this study relies on labeled data to differentiate yellow and green points on trees, necessitating manual inputs from various time points. It's important to note that this algorithm might require calibration between different years and across tree varieties for optimal performance.

4. Conclusion and Future Work

Leaf Nitrogen concentration is one of the critical factors that determines the quality of fruits and the overall health of the apple trees. Growers often rely on different visual cues including the color of the canopy for assessing plant health and nitrogen requirements. This study presented a machine vision-based solution for quantitatively assessing the color of the canopy. Specifically, this study segmented the test tree in a natural background using point clouds, identified yellow and green regions in the canopy, and used a metric called *yellowness index* to quantify the yellowness of the trees. It was found that the yellowness of the tree depended on the leaf nitrogen concentrations with higher nitrogen areas having a greener canopy and lower nitrogen areas having a yellower canopy. The trees notably began transitioning in color around the 29th week following full bloom in both years the test was conducted. The trees with lower and higher nitrogen showed the highest significant differences between the *yellowness indices* during week 4 (Nov. 4) during 2021 and week 2 (Oct. 27) and week 4 (Nov. 10) during 2023. The difference in these dates signifies the importance of other factors like temperature, humidity, and growing degree days during different years to predict tree nitrogen levels from the color change pattern. Overall, the findings from this study could be summarized as:

1. A machine vision-based system could be used to segment the yellow and green foliage in the trees. The metric *yellowness index* was defined to quantify the "yellowness" in the trees. Two algorithms were proposed and the best performing one was chosen based on

performance on the validation dataset. The algorithm was able to predict the *yellowness index* of the regions with a R^2 value of 0.72.

2. The *yellowness index* of the trees was found to correlate with the leaf nitrogen levels in the trees. Trees with different nitrogen levels showed different yellowing patterns. Critical dates during both years of the study were identified based on ANOVA analysis followed by posthoc tests. The yellowness values at critical weeks could be a good variable to identify the trees with low and high nitrogen levels.

This study presented a unique way of assessing the color of the canopies and explored its relationship with leaf Nitrogen concentration. This method could be a good alternative to traditional methods like chemical methods, chlorophyllmeter, and spectral analysis and can give instantaneous results. The study also provided critical insights into the fall color changes in apple trees and their relationship with leaf nitrogen concentrations.

The study provides precise tree level information and the data could be collected using any ground vehicle. One major limitation of this study to assess the leaf nitrogen level for the tree is that some years, the tree might freeze and never show the color change. In such cases, it is important to not rely on just a single factor and have a decision support system that takes multiple features as input, making the decision more robust. The *yellowness index* values along with other commonly used visual features like canopy density, trunk cross-sectional area, and shoot length can be combined into a single robust model and could aid in developing a robust decision support system for efficient fertilization plans tailored to individual tree nitrogen needs.

For practical implementation, machinery capable of delivering nutrients at a per-tree level becomes essential. Private companies like Monarch Tractor, USA (Cooley, 2022); Robotics Plus, NZ(Uys, 2022); and Burrows Tractor, USA (Milkovich, 2023) or academic institutions like Washington State University (Munir, 2023), are currently focusing on autonomous operations in orchards, with precise orchard localization. Integrating the insights from this

study into such machinery would provide a comprehensive solution for growers. Achieving per-tree precision could significantly enhance tree health, fruit quality, and ultimately increase orchard profits.

Acknowledgement

This research was supported by the Washington Tree Fruit Research Commission. Special thanks to David Allan, Bernardita Sallato, and Dr. Matthew D. Whiting for providing valuable feedback and support during this work.

References

- Aggelopoulou, K., Pateras, D., Fountas, S., Gemtos, T., Nanos, G., 2011. Soil spatial variability and site-specific fertilization maps in an apple orchard. *Precision Agriculture* 12, 118–129.
- Aggelopoulou, K., Wulfsohn, D., Fountas, S., Gemtos, T., Nanos, G., Blackmore, S., 2010. Spatial variation in yield and quality in a small apple orchard. *Precision agriculture* 11, 538–556.
- Aguñera, E., Cabello, P., De La Haba, P., 2010. Induction of leaf senescence by low nitrogen nutrition in sunflower (*helianthus annuus*) plants. *Physiologia plantarum* 138, 256–267.
- AgWeatherNet, . Wheat grain gdds. URL: <https://smallgrains.wsu.edu/weather-resources/wheat-grain-growing-degree-day-calculator/>.
- Ali, M., Al-Ani, A., Eamus, D., Tan, D., 2012. Leaf nitrogen determination using handheld meters, in: Australian Agronomy Conference.
- Arno, J., Martínez-Casasnovas, J.A., Uribeetxebarria, A., Escola, A., Rosell-Polo, J.R., 2017. Comparing efficiency of different sampling schemes to estimate yield and quality parameters in fruit orchards. *Advances in Animal Biosciences* 8, 471–476. doi:[10.1017/S2040470017000978](https://doi.org/10.1017/S2040470017000978). publisher: Cambridge University Press.

- Baret, F., Fourty, T., 1997. Radiometric estimates of nitrogen status of leaves and canopies, in: Diagnosis of the nitrogen status in crops. Springer, pp. 201–227.
- Bartlett, P., Freund, Y., Lee, W.S., Schapire, R.E., 1998. Boosting the margin: A new explanation for the effectiveness of voting methods. *The annals of statistics* 26, 1651–1686.
- Cheng, L., 2010. When and how much nitrogen should be applied in apple orchards. *New York Fruit Quarterly* 18, 25–28.
- Cheng, L., Schupp, J., 2004a. Nitrogen fertilization of apple orchards. *New York fruit quarterly* 12, 22–25.
- Cheng, L., Schupp, J., 2004b. Nitrogen fertilization of apple orchards .
- Cho, S.E., 2010. Probabilistic assessment of slope stability that considers the spatial variability of soil properties. *Journal of geotechnical and geoenvironmental engineering* 136, 975–984.
- Cooley, B., 2022. The first smart electric tractor makes more sense than cars with the same tech. URL: <https://www.cnet.com/roadshow/news/i-thought-i-knew-why-theyre-making-electric-tractors-i-didnt/>.
- Ferguson, I.B., Triggs, C.M., 1990. Sampling factors affecting the use of mineral analysis of apple fruit for the prediction of bitter pit. *New Zealand Journal of Crop and Horticultural Science* 18, 147–152. doi:[10.1080/01140671.1990.10428086](https://doi.org/10.1080/01140671.1990.10428086).
- De la Haba, P., De la Mata, L., Molina, E., Aguñera, E., 2014. High temperature promotes early senescence in primary leaves of sunflower (*helianthus annuus* l.) plants. *Canadian Journal of Plant Science* 94, 659–669.
- James A. Taylor, John-Paul Praat, A. Frank Bollen, 2007. Spatial Variability of Kiwifruit Quality in Orchards and Its Implications for Sampling and Mapping in: *HortScience* Volume 42 Issue 2 (2007) URL: <https://doi.org/10.21273/HORTSCI.42.2.246>.

- Kang, C., Diverres, G., Achyut, P., Karkee, M., Zhang, Q., Keller, M., 2023. Estimating soil and grapevine water status using ground based hyperspectral imaging under diffused lighting conditions: Addressing the effect of lighting variability in vineyards. *Computers and Electronics in Agriculture* 212, 108175.
- Kim, C., Kim, S.J., Jeong, J., Park, E., Oh, E., Park, Y.I., Lim, P.O., Choi, G., 2020. High ambient temperature accelerates leaf senescence via phytochrome-interacting factor 4 and 5 in arabidopsis. *Molecules and cells* 43, 645.
- Kirk, P.L., 1950. Kjeldahl method for total nitrogen. *Analytical chemistry* 22, 354–358.
- Klein, I., Levin, I., Bar-Yosef, B., Assaf, R., Berkovitz, A., 1989. Drip nitrogen fertigation of 'starking delicious' apple trees. *Plant and soil* 119, 305–314.
- Lee, D.W., 2002. Anthocyanins in autumn leaf senescence .
- Li, C., Guo, C., Han, L., Jiang, J., Cheng, M.M., Gu, J., Loy, C.C., 2021a. Low-light image and video enhancement using deep learning: A survey. *IEEE transactions on pattern analysis and machine intelligence* 44, 9396–9416.
- Li, C., Guo, C., Loy, C.C., 2021b. Learning to enhance low-light image via zero-reference deep curve estimation. *IEEE Transactions on Pattern Analysis and Machine Intelligence* 44, 4225–4238.
- Li, W., Zhu, X., Yu, X., Li, M., Tang, X., Zhang, J., Xue, Y., Zhang, C., Jiang, Y., 2022. Inversion of nitrogen concentration in apple canopy based on uav hyperspectral images. *Sensors* 22, 3503.
- Ma, X., Feng, J., Guan, H., Liu, G., 2018. Prediction of chlorophyll content in different light areas of apple tree canopies based on the color characteristics of 3d reconstruction. *Remote Sensing* 10, 429.

Mahmud, M.S., Zahid, A., He, L., Choi, D., Krawczyk, G., Zhu, H., Heinemann, P., 2021. Development of a lidar-guided section-based tree canopy density measurement system for precision spray applications. *Computers and Electronics in Agriculture* 182, 106053.

Majid, I., Khalil, A., Nazir, N., Majid, I., 2018. Economic analysis of high density orchards. *International Journal of Advance Research in Science & Engineering* 7, 821–9.

Milkovich, M., 2023. Steering into the future with autonomous tractor technology. URL: <https://www.goodfruit.com/steering-into-the-future-with-autonomous-tractor-tech-video/>.

Munir, S., 2023. Washington state university utilizes warthog to improve nitrogen management in orchards. URL: <https://clearpathrobotics.com/blog/2023/08/washington-state-university-utilizes-warthog-to-improve-nitrogen-management-in-orchar>

Murneek, A.E., Logan, J., 1932. Autumnal migration of nitrogen and carbohydrates in the apple tree with special reference to leaves. University of Missouri, College of Agriculture, Agricultural Experiment Station.

Naschitz, S., Naor, A., Wolf, S., Goldschmidt, E.E., 2014. The effects of temperature and drought on autumnal senescence and leaf shed in apple under warm, east mediterranean climate. *Trees* 28, 879–890.

Natekin, A., Knoll, A., 2013. Gradient boosting machines, a tutorial. *Frontiers in neurorobotics* 7, 21.

NationalGeographic. Chlorophyll. <https://education.nationalgeographic.org/resource/chlorophyll/>. (Accessed on 12/26/2023).

Neilsen, D., Neilsen, G., 2002. Efficient use of nitrogen and water in high-density apple orchards. *HortTechnology* 12, 19–25.

- Neilsen, G.H., Neilsen, D., Herbert, L., 2009. Nitrogen fertigation concentration and timing of application affect nitrogen nutrition, yield, firmness, and color of apples grown at high density. *HortScience* 44, 1425–1431.
- Parkin, T., 1993. Spatial variability of microbial processes in soil—a review. *Journal of environmental quality* 22, 409–417.
- Paudel, A., Davidson, J.R., Grimm, C., Karkee, M., 2023. Vision-based normalized canopy area estimation for variable nitrogen application in apple orchards. *Smart Agricultural Technology* 5, 100309.
- Paudel, A., Karkee, M., Davidson, J.R., Grimm, C., 2022. Canopy density estimation of apple trees. *IFAC-PapersOnLine* 55, 124–128.
- Putra, B.T.W., Soni, P., 2020. Improving nitrogen assessment with an rgb camera across uncertain natural light from above-canopy measurements. *Precision Agriculture* 21, 147–159.
- Quigley, M., Gerkey, B., Conley, K., Faust, J., Foote, T., Leibs, J., Berger, E., Wheeler, R., Ng, A., 2009. Ros: an open-source robot operating system, in: *Proc. of the IEEE Intl. Conf. on Robotics and Automation (ICRA) Workshop on Open Source Robotics*, Kobe, Japan.
- Raese, J.T., Drake, S.R., Curry, E.A., 2007. Nitrogen fertilizer influences fruit quality, soil nutrients and cover crops, leaf color and nitrogen content, biennial bearing and cold hardiness of ‘golden delicious’. *Journal of plant nutrition* 30, 1585–1604.
- Rallo, L., Barranco, D., Castro-García, S., Connor, D.J., Gómez del Campo, M., Rallo, P., 2013. High-density olive plantations. *Horticultural Reviews Volume 41* , 303–384.
- Rorie, R.L., Purcell, L.C., Karcher, D.E., King, C.A., 2011. The assessment of leaf nitrogen in corn from digital images. *Crop Science* 51, 2174–2180.

Sallato, B., 2017. Leaf tissue analysis. URL: <https://treefruit.wsu.edu/orchard-management/soils-nutrition/leaf-tissue-analysis/>.

Sanchez, E.E., Khemira, H., Sugar, D., Righetti, T., 1995. Nitrogen management in orchards.

Shi, P., Wang, Y., Xu, J., Zhao, Y., Yang, B., Yuan, Z., Sun, Q., 2021. Rice nitrogen nutrition estimation with rgb images and machine learning methods. *Computers and Electronics in Agriculture* 180, 105860.

Spencer, P.W., 1973. Apple leaf senescence: leaf disc compared to attached leaf. *Plant physiology* 51, 89–92.

Stereolabs, 2023. stereolabs/zed-ros-wrapper. URL: <https://github.com/stereolabs/zed-ros-wrapper>. original-date: 2015-09-09T14:29:32Z.

Thompson, D., 2017. How to Use Color Spaces to Talk About Color - First Source Worldwide. URL: <https://www.fsw.cc/color-spaces/>.

Treder, W., Klamkowski, K., Kowalczyk, W., Sas, D., Wojcik, K., et al., 2016. Possibilities of using image analysis to estimate the nitrogen nutrition status of apple trees. *ZemdirbysteAgriculture* 103, 319–326.

Umali, B.P., Oliver, D.P., Forrester, S., Chittleborough, D.J., Hutson, J.L., Kookana, R.S., Ostendorf, B., 2012. The effect of terrain and management on the spatial variability of soil properties in an apple orchard. *Catena* 93, 38–48.

UniversityofArizona, . Nitrogen management guide for apples. URL: <chrome-extension://efaidnbmnnnibpcajpcglclefindmkaj/https://ag.arizona.edu/crop/soils/aznapples.pdf>.

Upadhyaya, P., Karkee, M., Kshetri, S., Paudel, A., 2023. Automated lag-phase detection in wine grapes using a mobile vision system. *Smart Agricultural Technology* , 100381.

- Uys, G., 2022. Robotics plus launches unmanned hybrid vehicle that solves labour issues. URL: <https://www.stuff.co.nz/business/farming/130353006/robotics-plus-launches-unmanned-hybrid-vehicle-that-solves-labour-issues>.
- Wachs, J.P., Stern, H.I., Burks, T., Alchanatis, V., 2010. Low and high-level visual featurebased apple detection from multi-modal images. *Precision Agriculture* 11, 717–735.
- Van der Walt, S., Schönberger, J.L., Nunez-Iglesias, J., Boulogne, F., Warner, J.D., Yager, N., Gouillart, E., Yu, T., 2014. scikit-image: image processing in python. *PeerJ* 2, e453.
- Wang, T., Sankari, P., Brown, J., Paudel, A., He, L., Karkee, M., Thompson, A., Grimm, C., Davidson, J., Todorovic, S., 2023. Automatic estimation of trunk cross sectional area using deep learning. Collaborative Robotics & Intelligent Systems Institute, Oregon State University .
- Wang, Z., Underwood, J., Walsh, K.B., 2018. Machine vision assessment of mango orchard flowering. *Computers and Electronics in Agriculture* 151, 501–511.
- Wen, X., Zhu, X., Cao, S., Guo, X., Yu, R., Xiong, J., Gao, D., 2018. Nitrogen estimation model of apple leaves based on imaging spectroscopy. *Remote Sensing Science* 6.
- Wingler, A., Masclaux-Daubresse, C., Fischer, A.M., 2009. Sugars, senescence, and ageing in plants and heterotrophic organisms. *Journal of experimental botany* 60, 1063–1066.
- Wulfsohn, D., Aravena Zamora, F., Potin T´ellez, C., Zamora Lagos, I., Garc´ia-Fin˜ana, M., 2012. Multilevel systematic sampling to estimate total fruit number for yield forecasts. *Precision Agriculture* 13, 256–275. URL: <https://doi.org/10.1007/s11119-011-9245-2>, doi:10.1007/s11119-011-9245-2.
- Ye, X., Abe, S., Zhang, S., 2020. Estimation and mapping of nitrogen content in apple trees at leaf and canopy levels using hyperspectral imaging. *Precision Agriculture* 21, 198–225.

Zhang, S., Zhang, Y., Jiang, Z., Zou, D., Ren, J., Zhou, B., 2020. Learning to see in the dark with events, in: Computer Vision–ECCV 2020: 16th European Conference, Glasgow, UK, August 23–28, 2020, Proceedings, Part XVIII 16, Springer. pp. 666–682.

Zhang, Y., Guo, X., Ma, J., Liu, W., Zhang, J., 2021. Beyond brightening low-light images. International Journal of Computer Vision 129, 1013–1037.

Zhou, Q.Y., Park, J., Koltun, V., 2018. Open3d: A modern library for 3d data processing. arXiv preprint arXiv:1801.09847 .